E-proceedings of the 36th IAHR World Congress
28 June – 3 July, 2015, The Hague, the Netherlands

APPLICATION OF FLEXIBLE RING NET BARRIERS TECHNOLOGY FOR DEBRIS FLOW CONTROL IN SAN MARTIN TORRENT – AYACUCHO - PERU

JOEL ORE IWANAGA[(1)]

[(1)] *Maccaferri. Lima, Peru*
joel.iwanaga@maccaferri.com.pe; joeliwanagaore@gmail.com

ABSTRACT

On December 2009 in Ayacucho, heavy rainfall were recorded in Killari and Emadi stations, with a time interval of 1 minute, reaching intensities of the order of 182.80 mm/hr and 164.60 mm/hr and total rainfall of 52.80 mm and 34.00 mm in just 115 minutes, respectively, the same that caused the transit of the excessive hydrograph generating the transport of mud and stones to the historic downtown on San Martin Avenue. In the present investigation the model FLO 2D is used, which will determine the volume of sediment transport, and the main hydraulic characteristics corresponding to velocity and depth, allowing determine the design of the flexible barrier and the spacing along the torrent San Martin.

Keywords: *Mud flow, flexible barriers, FLO 2D*

1. INTRODUCTION

The problems generated by the transport of debris flow are usually unforeseen, mostly caused by heavy rains that achieved saturate the soil and subsequently cause excessive sediment transport to finally reach downstream villages, causing flooding and destruction. Today, there are alternatives, one of which corresponds to the flexible barriers that still is not widespread in our country, but undoubtedly is an alternative to retain small volumes of sediment (Wendeler et al., 2008). This solution is used in the present investigation, as an alternative, to mitigate the possible volumes of debris that could develop in the future, given the negative history of heavy rains that occurred in December 2009, where a large amount of sludge and stones is transported from the top of the San Martin torrent, the same which came to the historic center of the city of Ayacucho, killing 11 people.

1.1 Debris flow

A typical debris flow is a torrential flow of a mixture of water, mud and debris that suddenly pushes forward a huge amount of mud and boulders (Figure 1). Certainly it is a natural phenomenon that not only cause disasters but also interested many researchers to interpret the nature of their behavior (Montenegro, 2014).

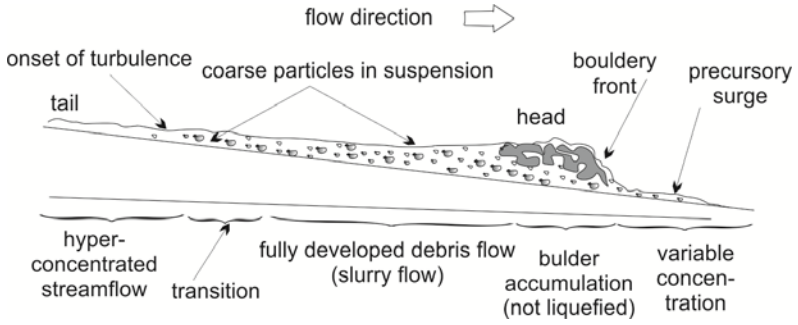

Figure 1. Typical schematic section of a debris flow (Diagram Pierson, 1986).

The debris flow is studied from the torrential hydraulics, the same that is the flood routing wherein the solids transport is so great and should be aware that the solid phase that forming part of this hyperconcentrated flow, cannot be separated from the water flow on the one hand with their equations of motion, and solid transport by the other hand (Montenegro, 2014). The modeling of debris flow is realized from the solution of the equations of Saint Venant, incorporating the rheology of the material in such a way to transit the flood to two dimensional level, and determine the hydraulic characteristics: speed, depth between other parameters that allow the design of the flexible structure.

1.2 Flexible barriers

Flexible barriers are structures that are generally positioned in a natural stream, the same that have V-shape, whose main characteristics are shown in Figure 2.

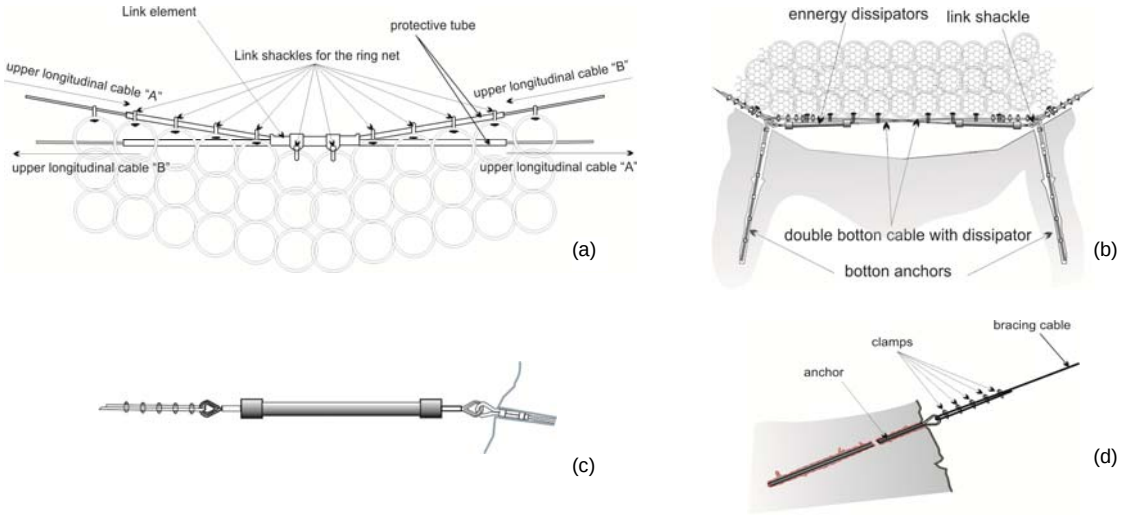

Figure 2. V-barrier system against debris flow: (a) Upper longitudinal cables. (b) Lateral and bottom cables. (c) Energy dissipating device. (d) Connection between anchor and bracing cable.

An advantage of ring net barriers is that they are light and flexible and can easily be installed in remote regions (Wendeler et al., 2008), these include the following components (Grimod, 2014):

- Transversal longitudinal cables, the sames that are able to transfer the forces developed by the hyperconcentrated flow from the interception structure to the lateral anchors;
- Interception structure, which is a rockfall mesh (generally ring nets panels) held up by the upper longitudinal cables and fixed to the lower longitudinal and lateral cables;
- Energy dissipators (brakes) allows the extension of the cables and consequently the forces acting on the anchors are reduced;
- Lateral anchors, which are composed of a double-leg flexible cable. They are installed in a drilled hole and fully grouted. They transfer the forces from the barrier to the ground.

2. CHARACTERIZATION OF WATERSHED STUDY

2.1 Geological and geomorphological characteristics

The San Martin torrent, is located northwest of the city of Ayacucho, and originates in the highlands of Mount Picota (Figure 3), which is a tributary of the Alameda river, crossing practically the Ayacucho city. This city is covered by sedimentary geological formations such as volcanic tuffs and tuffaceous sandstones, volcanic rocks such as lava and pyroclastic, Pleistocene deposits such as conglomerates and strongly cemented soils lacustrine, diatomite and recent deposits, such as colluvial, alluvial and fluvial, whose ages range between the upper tertiary and recent quaternary.

The Mount Picota, where he is seated the San Martin torrent, has a soil classified like well-graded silty sand gravel from ancient sedimentary origin (Pleistocene conglomerate) from regular soil geotechnical conditions.

Figure 3. San Martin torrent (SMT): (a) Top of San Martin torrent. (b) View of Ayacucho city from Mount Picota.

The main geomorphological characteristics of the San Martin torrent, are shown in Table 1.

Table 1. Main morphological features of San Martin Torrent.

FEATURE	VALUE
AREA (KM^2)	0.20
MAX. HEIGHT (M)	3219
MIN. HEIGHT (M)	2740
CATCHMENT AVERAGE SLOPE (°)	32
MAIN STREAM LENGTH (M)	1810
MAIN STREAM AVERAGE SLOPE (RURAL AREA - °)	20
MAIN STREAM AVERAGE SLOPE (URBAN AREA - °)	7.5
OUTCROPPING AREAS (CATCHMENT AREA - %)	30
LANDSLIDES AREAS (CATCHMENT AREA - %)	15

2.2 Hyetograph and design hydrograph

To develop the design of the flexible barrier, be taken into account the rainfalls occurred on 16 December 2009, with the same that will be determines design precipitation hyetograph from the inverse-distance-square method, which has incidence in the basin of the San Martin torrent. In Figure 4, the rains in the Killari and Emadi stations, as well as the watershed of the San Martin torrent is shown.

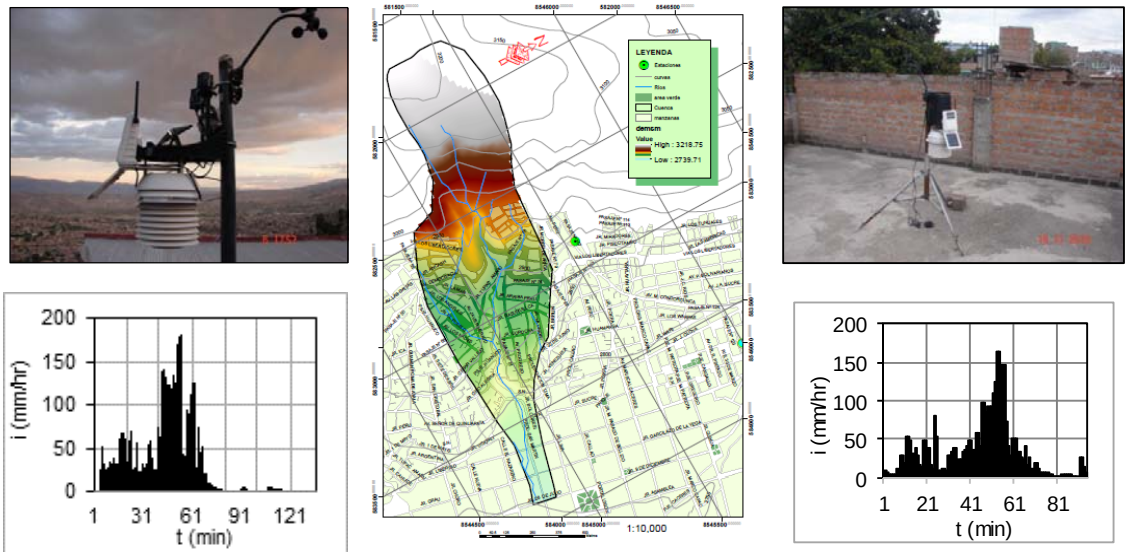

Figure 4. Hyetographs total rainfall recorded in the city of Ayacucho: (a) Killari Station. (b) Emadi Station.

In Figure 5 is shown, the hietograma and design hydrograph for the day December 16, date on which occurred the disaster of debris transport in the city of Ayacucho, from the creek San Martin. The design hydrograph is determined from the Clark unit hydrograph, considering a time of concentration equal to 0.13 hr, storage coefficient of 0.16 hr and for determining infiltration rates a number of curve 67 (Oré, 2014).

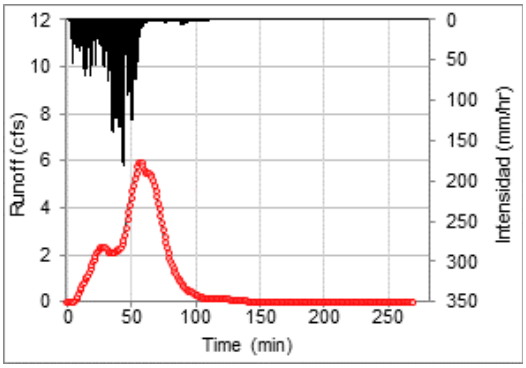

Figure 5. Hyetograph and design hydrograph.

3. DESCRIPTION OF SEDIMENT TRANSPORT MODEL

To model the transport of sediment, it is will be used the FLO 2D numerical model extensively validated worldwide (Pirulli, 2008), from same that it is described their equations of continuity and momentum to develop the two dimensional flow routing:

$$\frac{\partial h}{\partial t}+\frac{\partial\left(h\overline{v_x}\right)}{\partial x}+\frac{\partial\left(h\overline{v_y}\right)}{\partial y}=i \qquad [1]$$

$$S_{fx}=S_{ox}-\frac{\partial h}{\partial x}-\frac{\overline{v_x}}{g}\frac{\partial h\overline{v_x}}{\partial x}-\frac{\overline{v_y}}{g}\frac{\partial \overline{v_x}}{\partial y}-\frac{1}{g}\frac{\partial \overline{v_x}}{\partial t} \qquad [2]$$

$$S_{fy}=S_{oy}-\frac{\partial h}{\partial y}-\frac{\overline{v_y}}{g}\frac{\partial h\overline{v_y}}{\partial y}-\frac{\overline{v_x}}{g}\frac{\partial \overline{v_y}}{\partial x}-\frac{1}{g}\frac{\partial \overline{v_y}}{\partial t} \qquad [3]$$

Where: $S_f=\frac{\tau_y}{\gamma_m h}+\frac{K\eta V}{8\gamma_m h^2}+\frac{n^2V^2}{h^{4/3}}$ denotes the depth-averaged flow velocity, h is the flow depth, i is the rainfall intensity on the flow surface and g is the gravity constant. The friction slope components S_{fx} y S_{fy} are written as functions of the bed slope S_{ox} y S_{oy}, the pressure gradient and the convective and local acceleration terms. FLO 2D adopts a quadratic rheological approach and the friction slope is therefore provided by the following expression:

$$S_{fi(i=x,y)}=\frac{\tau}{\rho g h}=\frac{\tau_y}{\rho g h}+\frac{K\eta\overline{v_i}}{8\rho g h^2}+\frac{n_{td}^2\overline{v_i}^2}{h^{4/3}} \qquad [4]$$

where τ is the shear stress, τ_y is the Bingham yield stress, η is the Bingham viscosity, K is the flow resistance parameter and n_{td} is the equivalent Manning coefficient for the turbulent and dispersive shear stress components.

The first and the second terms on the right hand side of Eq. [4] are, respectively, the yield term and the viscous term as defined in the Bingham equation. The last term represents the turbulence contribution.

4. METHODOLOGY OF DESIGN OF FLEXIBLE BARRIER

For the dimensioning of the flexible barrier is must considered three types of load that condition the stability of the barrier in a torrent when passes a debris flow: dynamic load, loading due to debris overtopping and static load considering in this last case the time instants required for determining the height of the sediment accumulation (Grimod, 2014). Figure 6 shows the variables to consider in the design of the flexible barrier, considered for a time $t=0$ y un $t>0$.

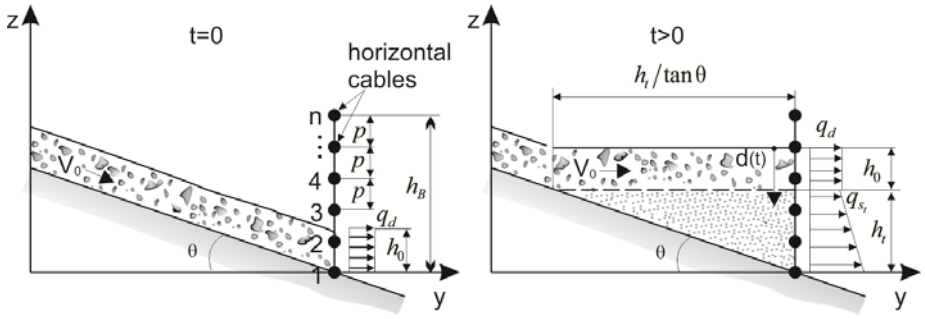

Figure 6. Accumulation of debris flow at different times.

4.1 Dynamic load calculation

The maximum dynamic load is determined from the following formula:

$$q_{d_{\max}}=\alpha\rho_d v_0^2 \quad (KPa) \qquad [5]$$

Donde $\alpha=2$ is an empirical coefficient for dynamic loads (GEO, 2011), $\rho_d\left(Kg/m^3\right)$ is the mass density of debris and $v_0\left(m/s\right)$ is the impact velocity of debris.

To determine dynamic load with incidence in each of the cables is taken into account the height of the flow χ_i, corresponding to the minimum value among h_i y p, described below:

$$q_{di} = \alpha \rho_d v_0^2 \chi_i \quad (KPa) \qquad [6]$$

Where: $\chi_i = \min(h_i, p)$ y $h_i = h_0 \frac{L_1}{L_i}$, $h_i(m)$ is a parameter relating the depth flow $h_0(m)$ to the lengths of the i^{th} cable with respect to length of the cable 1, $p = \frac{h_B}{n-1}(m)$ is the spacing between cables, where n is the number of cables that make up the barrier. Note that the height of the flow to the cables ends is equal to half of the value obtained.

4.2 Loading due to debris overtopping

In Figure 7, the height of debris flow bypass is shown, the same that generates a hydraulic head on the last cable, determined as follows:

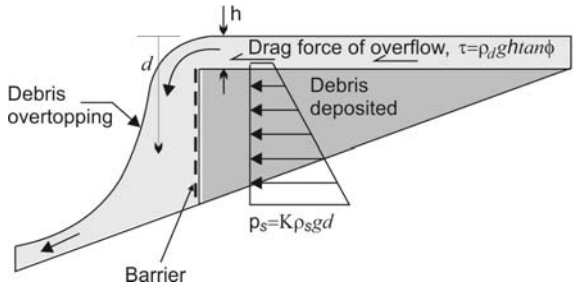

Figure 7. Flow passage through the last cable.

$$q_\tau = \tau L \quad (KN/m) \qquad [7]$$

Where:

$$\tau = \rho_d g h_N \left[\tan\phi + \frac{v_0^2}{\varepsilon h_0} \right] \quad (KPa) \qquad [8]$$

$$L = \frac{h_B}{tg\left(45 + \frac{\phi}{2}\right)} \quad (m) \qquad [9]$$

In the above equations $\tau(KPa)$ is the drag force of overflow, $g(m/s^2)$ is the gravity, $h_N(m)$ is the height of flow on top, $v_0(m/s)$ is the impact velocity of debris, ϕ is the apparent friction angle, $\varepsilon(m/s^2)$ is the turbulence coefficient, $h_B(m)$ is the height of the barrier.

This load due to debris-flow bypass must be added to the static load on the last cable.

4.3 Static load calculation

For the determination of the static load q_{s_i}, which has an impact on each of the cables i, is necessary to determine heights measured from the surface of debris flow, the same it is variable depending on the time and K, that it is the active earth pressure coefficient, for which the following formula is used:

$$q_{si} = K d_i \rho_d g p = K\left(h_i + h_t - h_B \frac{i-1}{n-1}\right)\rho_d g p \quad (KPa) \qquad [11]$$

Where $K = \frac{1-sin\phi}{1+sin\phi} \geq 0.5$ is the active earth pressure coefficient, the heights h_i were determined above as part of the equation [6], the same varies for each cable and the height h_t, is calculated, taking into account the time of debris flow accumulation on the last cable to the most critical situation, taking account the height from $z_i = z_{i-1} + p$:

$$t_N = \frac{z_N^2}{2v_0 h_0 \tan\theta} \text{ (seg)} \qquad [12]$$

Where z_N is the height of load on the last cable. Then determine for different times t_i ,the height of accumulation, taking into account as limit the accumulation time of the last cable t_N :

$$h_{ti} = \sqrt{2v_0 t_i h_0 \tan\theta} \text{ (m)} \qquad [13]$$

Finally determine the loads from the equation [11], for each of the cables in each of the selected time, taking into account that the static load last cable, must be add the load due to debris overtopping (equation [7]). In Figure 8, is shown as load heights h_{t_i} , only have influence on some loads on the cables, unlike height h_{t_N} , which has implications for all cables.

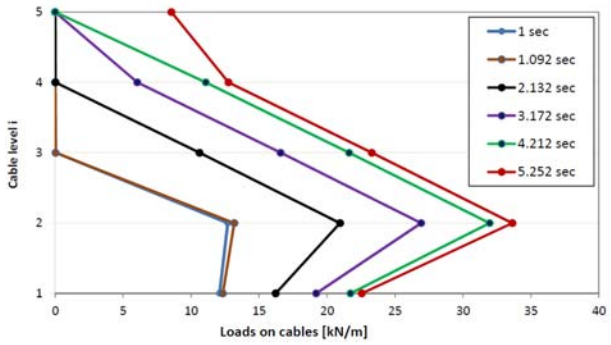

Figura 8. Static loading on cables at different time intervals (KN/m)

4.4 Calculation of the maximum design load on each of the cables.

To determine the maximum design loads in each of the cables, one must compare the static loads (to t_N) with the dynamic loads, considering Figure 9, Where is shown the acting loads and the deformation of the cable i .

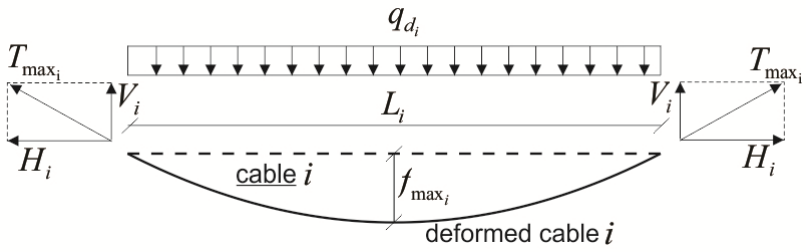

Figure 9. Plan view with the forces acting on the generic deformed cable.

Must perform the following procedure to determine the displacement of the brakes of each of the cables and checking that the tension exerted on each of the cables is less than 10 KN.

1. Assume the maximum sag f_{max_i} , of the cable i ;
2. Calculate the curvature radius of the sag;

$$R = \sqrt{\left(\frac{L_i}{2}\right)^2 + 0.25\left(\frac{L_i^2}{4f_{max_i}} + f_{max_i} - \frac{L_i^2}{2f_{max_i}}\right)^2} \ (m) \qquad [14]$$

Where L_i : width of the cable i before deforming.

3. Calculate the angle β formed by the radius with respect to $L_i/2$;

$$\beta = \arcsin\frac{L_i}{2R} \quad [15]$$

4. Calculate the length of deformation L_f ;

$$L_f = 2R\theta \ (m) \quad [16]$$

5. Calculate the brake elongation $\Delta L = L_b$

$$\Delta L = L_b = L_f - L_i \ (m) \quad [17]$$

6. Enter to the Figure 10 with ΔL and determine the tensile strength $T_b \ (KN)$.

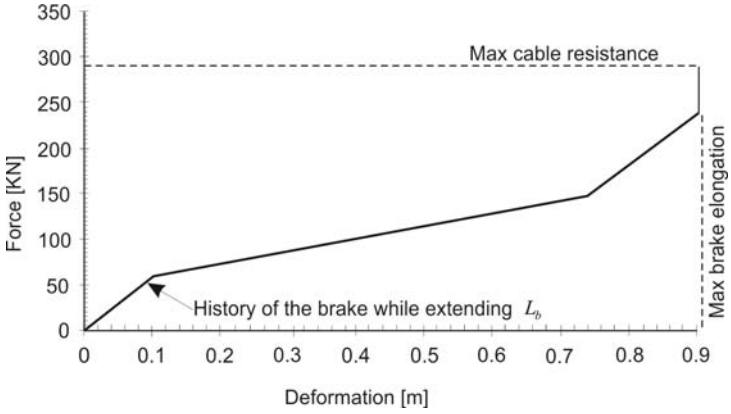

Figure 10. Load vs deformation on the transversal cable.

7. Due to the deformation of the brake, the stress on the cables is reduced (Grimod, 2014). According to the graph of Figure 10, the energy dissipater device constantly deforms until the axial force on the rope reaches the maximum force applied on the energy dissipater. The maximum load $T_{\max_i}$ acting on the cable i^{th} can be calculated:

$$T_{\max_i} = \sqrt{V_i^2 + H_i^2} \ (KN) \quad [18]$$

Where: V_i and H_i are the maximum loads acting on the cable i^{th} respectively in the directions parallel and transversal to flow direction (Figure 9). They are defined as following:

$$V_i = \frac{q_{\max_i} L_i}{2} \ (KN) \quad [19]$$

$$H_i = \frac{q_{\max_i} L_i^2}{8 f_{\max_i}} \ (KN) \quad [20]$$

Where the load $q_{\max_i}$ is determined from the following equations:

$$q_{\max i} = \max\left(q_{si} * p; q_{di} * \min\left(p, h_0\right)\right) \ (KN/m) \quad [21]$$

$$q_{\max N} = \max\left(q_{si} * p; q_{di} * \min\left(p/2, h_0\right)\right) + q_\tau \ (KN/m) \quad [22]$$

The maximum design tension is determined, considering the number of cables in each level of cable, for example if the level had two cables, then the maximum design tension is determined from:

$$T_{\max_{diseño_i}} = \frac{T_{\max_i}}{2} \ (KN) \quad [23]$$

8. Calculate $\Delta T_{\max} = T_{\max_{diseño_i}} - T_b$

9. If $\Delta T_{\max} > 10KN$, then assume another $f_{\max_i}$ and return to item 1 and repeat the process until that $\Delta T_{\max} < 10KN$.

5. RESULTS AND DISCUSSION

It has made the design of the flexible barrier, taking into account the results from the program FLO 2D with respect to depth and maximum speed. These values are equal to 0.6 m and 4.6 m / s, respectively, as a response to the hydrograph presented in Figure 11.

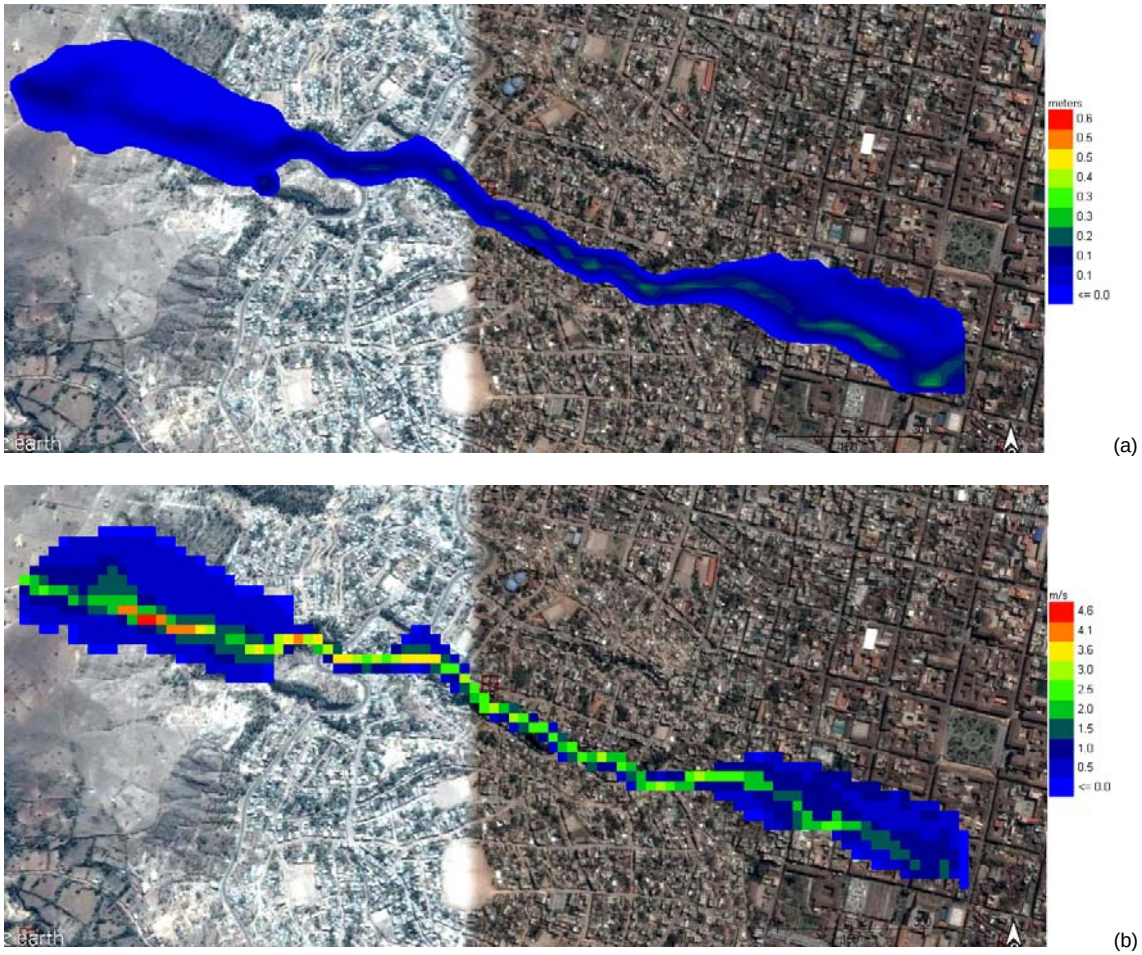

Figure 11. Results (a) maximum depth and (b) speed.

The design has been made of the flexible barrier, the same as shown below in Table 2, for each cable, observing the maximum displacement of the energy dissipation and safety factors.

Table 2. Results of sizing from flexible barrier.

Cable N°	N° of cables	z_i (m)	$f_{\max_i}$ (m)	$q_{\max_i}$ (KN/m)	$\gamma_q T_{\max}$	T_{ult}/γ_M	SF
1	2	0.3	0.7	20.63	73.18	244	3.33
2	2	1.3	1.2	26.71	103.83	244	2.35
3	2	2.3	1.2	18.28	105.62	244	2.31
4	4	3.3	1	14.78	70.11	244	3.48

6. CONCLUSIONS

The numerical model presented in detail, allows the design of the flexible barrier, it takes into account the analysis of two-dimensional flow to routing debris flow, the speed and height as fundamental design parameters allow to design the flexible barrier. In this case the speed is equal to 4.6 m / s and the height of the flow is equal to 0.6 m.

One can see that you have maximum displacement of 1.20 m for the second and third cable level as well as the security factors greater than 2.

ACKNOWLEDGMENTS

The author acknowledges support from the National University of San Cristobal of Huamanga through which was obtained rainfall data design and the National University of Huancavelica who provided the software FLO 2D. Finally I would also like to thank the MACCAFERRI OF PERU Company, by providing relevant information on flexible barriers and sizing.

REFERENCES

GEO 2011. Design requirements for flexible Debris-resisting Barriers. *Geotechnical Engineering Office, Civil Engineering and Development Department.* The Government of the Hong Kong Special Administrative Region (Draft as at 12.10.2011).

Grimod A. (2014). Simplified methodology to design flexible debris flow barriers. *GEO Regina*, *67th Canadian Geotechnical Conference.*

Montenegro J. (2014). Estudio del flujo de detritos de Tamburco y gestión del riesgo. *IAHR XXV Congreso Latinoamericano de Hidráulica,* Santiago, Chile.

Oré J. (2014). Calibración lluvia escorrentía mediante modelos agregados y distribuidos Cuenca experimental Yanaccacca. *IAHR XXV Congreso Latinoamericano de Hidráulica,* Santiago, Chile.

Pirulli M. (2008). Assessing potential debris flow runout: a comparison of two simulation models. Nat. Hazards Earth Syst. Sci., 8, 961-971.

Wendeler C. Volkwein A. and Roth A. (2005). Field testing and numerical modeling of flexible debris flow barriers. http://www.wsl.ch/wsl/info/mitarbeitende/volkwein/pdf/8162.pdf.